

Exact description of photon migration in anisotropically scattering media

V. N. Fomenko,¹ F. M. Shvarts,² and M. A. Shvarts¹

¹*Department of Mathematics, University for Railway Communications, St. Petersburg, Russia*

²*State Optical Institute, Institute for Laser Physics, St. Petersburg, Russia*

(Received 30 September 1998)

The aim of the present paper is to deliver a method for exact calculation of the probability of photon migration in an infinite and homogeneous medium scattering photons anisotropically. The phase function is represented as an expansion over spherical harmonics. The probability of photon migration is obtained as an expansion with respect to the number of scatterings with the coefficients depending on the distance-to-time ratio and can be easily calculated from recurrence relations. Up to 30 scatterings are taken into account when computing the migration probabilities, the number of effectively contributing scatterings being strongly dependent on the distance-to-time ratio decreasing when one approaches the propagation front. The important property of the method is its capability to describe exactly migration from the early arriving photons up to the scattering ones. The limits of the approximate description of anisotropic scattering as isotropic with an effective value of the scattering coefficient is analyzed by calculating the best-fit value of the scattering coefficient.

PACS number(s): 42.68.Ay, 02.70.Lq, 05.60.-k, 87.63.-d

I. INTRODUCTION

Recently, optical tomography has become increasingly important in tissue investigations, in particular, those related to medical diagnostics. For purposes of optical tomography, a correct description of photon migration plays a fundamental role. In this paper, we give an exact theory of photon migration in an anisotropically scattering infinite medium. Nowadays, the diffusion approximation is widely used to describe photon migration. But the limits of this approximation are narrowed down by the fact that the most informative photons are the ones first to arrive, which form the propagation front and are not described by diffusion theory (see Refs. [1] and [2], for instance). For this reason, a method going beyond the diffusion limit is greatly desirable for tissue investigations. In this paper, we investigate the accuracy of the widely applied method of describing anisotropically scattering media as isotropically scattering media with an effective scattering coefficient. The conclusion we draw from this analysis is that such an approach is no more than a rough approximation if photons with small retardation are of interest. Note that the present paper is a natural generalization of the method describing photon migration in isotropically scattering media (see Ref. [3]). This paper is organized as follows: in Sec. II we give the mathematical apparatus of the theory, results of the numerical analysis of photon migration in anisotropically scattering media are given in Sec. III, and Sec. IV contains some concluding remarks.

II. FORMULATION OF THE THEORY

In this section, we give a theoretical description of photon propagation in an anisotropically scattering medium which is assumed to be homogeneous and isotropic. Let $P(\mathbf{r}, t)$ be the expectation value of the number of photons traveling from the initial space-time point $O(0,0)$ to a small volume ΔV around the final point $M(\mathbf{r}, t)$ per unit volume. In what follows we ignore any nonlinear optical effects, which implies a

low enough level of the radiation intensity. This restriction is compatible with many important applications, in particular, optical tomography. An important consequence of this assumption is that $P(\mathbf{r}, t)$ is a linear functional of the radiation flux at the initial point $R(\hat{\mathbf{n}})$:

$$P(\mathbf{r}, t) = \mathbb{P}(\mathbf{r}, t)[R(\hat{\mathbf{n}})], \quad (1)$$

where $\hat{\mathbf{n}}$ is a unit vector. Note that $P(\mathbf{r}, t)$ equals the migration probability density if $R(\hat{\mathbf{n}})$ is normalized to unity:

$$\int R(\hat{\mathbf{n}}) d\mathbf{n} = 1. \quad (2)$$

Equation (1) defines the functional \mathbb{P} on positive definite functions $R(\hat{\mathbf{n}})$. For what follows it is important to extend the functional \mathbb{P} to complex-valued functions. This can be done in a straightforward way using the linearity of \mathbb{P} . We affix the subscript n to the quantities \mathbb{P} and $P(\mathbf{r}, t)$ to indicate the number of scatterings the photon experiences on its migration. Figure 1 illustrates how to construct a recurrence relation for $P_n(\mathbf{r}, t)$. In this figure O and M are the initial and final points, respectively. The first scattering of the photon by the medium occurs at the point N . If the number of scatterings equals $n + 1$, then the migration on the segment NM contains n scatterings. We immediately arrive at the following relation:

$$P_{n+1}(\mathbf{r}, t)[R_O(\hat{\mathbf{n}})] = \int d^3r_1 P_n(\mathbf{r}_2, t - r_1)[R_N(\hat{\mathbf{n}}_1)], \quad (3)$$

where $R_O(\hat{\mathbf{n}})$ is the angle distribution of the radiation flux at the point O and $R_N(\hat{\mathbf{n}}_1)$ is the corresponding quantity at the point N per unit volume. Bearing in mind that the interior of the segment ON is the photon's free path, we have

$$R_N(\hat{\mathbf{n}}_1) = \frac{\exp[-(\mu_s + \mu_a)r_1]}{r_1^2} \mu_s f(\hat{\mathbf{n}}_1) R_O(\hat{\mathbf{r}}_1), \quad (4)$$

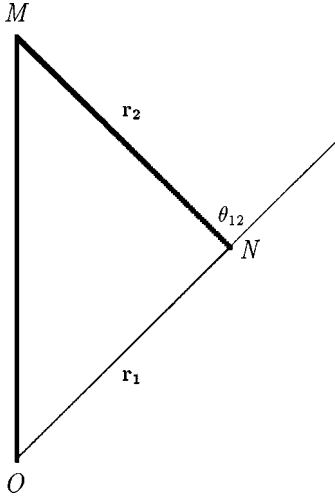


FIG. 1. Scheme explaining recursive description of photon migration.

where the light velocity is assumed to be unity, μ_s and μ_a are the scattering and absorption coefficients, respectively, and $f(\hat{\mathbf{n}}_1)$ is the phase function. Let us choose the polar axis along the vector $\hat{\mathbf{r}}_1$, which is the direction of the incident photons at the point N . Then the phase function can be expanded over spherical harmonics as follows:

$$f(\hat{\mathbf{n}}_1) = \sum_{\tilde{L}} \alpha_{\tilde{L}} \frac{Y_{\tilde{L}0}(\Omega_{\mathbf{r}_1})}{\sqrt{4\pi}}, \quad (5)$$

where $\Omega_{\mathbf{r}_1} = (\theta_1, \varphi_1)$; θ_1 is the angle between $\hat{\mathbf{n}}_1$ and \mathbf{r}_1 ; the angle φ_1 describes rotation with respect to the vector \mathbf{r}_1 . The normalization condition of the phase function $\int d\Omega f(\hat{\mathbf{n}}) = 1$ implies that $\alpha_0 = 1$. We obtain isotropic scattering if $\alpha_{\tilde{L}} = 0$ for $\tilde{L} > 0$. It is useful to expand $f(\hat{\mathbf{n}}_1)$ over spherical harmonics with respect to the vector $\hat{\mathbf{r}}_2$ as the polar axis. This yields

$$f(\hat{\mathbf{n}}_1) = \sum_{\tilde{L}M} \alpha_{\tilde{L}} D_{M0}^{\tilde{L}}(0, \theta_{12}, 0) \frac{Y_{\tilde{L}M}(\Omega_{\hat{\mathbf{r}}_2})}{\sqrt{4\pi}}, \quad (6)$$

where $D_{M0}^{\tilde{L}}$ is the Wigner function. After substituting expression (6) into Eq. (4) and using Eq. (3) and linearity of the functional P_n , we obtain

$$\begin{aligned} P_{n+1}(\mathbf{r}, t) [R_O(\hat{\mathbf{n}})] &= \int d^3r_1 \frac{\exp[-(\mu_s + \mu_a)r_1]}{r_1^2} \mu_s R_O(\hat{\mathbf{r}}_1) \\ &\times \sum_{\tilde{L}M} \alpha_{\tilde{L}} D_{M0}^{\tilde{L}}(0, \theta_{12}, 0) P_n(\mathbf{r}_2, t - r_1) \\ &\times \left[\frac{Y_{\tilde{L}M}(\Omega_{\mathbf{r}_2})}{\sqrt{4\pi}} \right]. \end{aligned} \quad (7)$$

We introduce the new quantity

$$P_n^{LM}(r, t) = P_n(\mathbf{r}, t) \left[\frac{Y_{LM}(\Omega_{\mathbf{r}})}{\sqrt{4\pi}} \right]. \quad (8)$$

We emphasize that \mathbf{r} in Eq. (8) is the polar axis for the spherical harmonic in the argument of $P_n(\mathbf{r}, t)$. Then setting $R_O(\hat{\mathbf{n}}) = (1/\sqrt{4\pi}) Y_{LM}(\Omega_{\mathbf{r}})$ in Eq. (7), one easily obtains

$$\begin{aligned} P_{n+1}^{LM}(r, t) &= \mu_s \int dr_1 d\Omega_{\mathbf{r}} \frac{1}{\sqrt{4\pi}} Y_{LM}(\Omega_{\mathbf{r}}) \\ &\times \exp[-(\mu_s + \mu_a)r_1] \\ &\times \sum_{\tilde{L}M} \alpha_{\tilde{L}} D_{M0}^{\tilde{L}}(0, \theta_{12}, 0) P_n^{\tilde{L}M}(r_2, t - r_1). \end{aligned} \quad (9)$$

The spherical harmonic in Eq. (9) depends on two angles, $\theta_1 = (\hat{\mathbf{r}}_1, \hat{\mathbf{r}})$ and φ_1 describes rotation with respect to the vector \mathbf{r} . The integrand in Eq. (9) depends on φ_1 only through $Y_{LM}(\Omega_{\mathbf{r}})$, and

$$\int_0^{2\pi} d\varphi_1 Y_{LM}(\Omega_{\mathbf{r}}) = 0$$

if $M \neq 0$. For this reason,

$$P_n^{LM}(r, t) = 0 \quad \text{for } M \neq 0. \quad (10)$$

As a result, Eq. (9) takes the form

$$\begin{aligned} P_{n+1}^L(r, t) &= \frac{\mu_s}{\sqrt{4\pi}} \int dr_1 d\Omega_{\mathbf{r}} Y_{L0}(\theta_1) \exp[-(\mu_s + \mu_a)r_1] \\ &\times \sum_{\tilde{L}} \alpha_{\tilde{L}} P_n^{\tilde{L}}(r_2, t - r_1) P_{\tilde{L}}(\cos \theta_{12}). \end{aligned} \quad (11)$$

In Eq. (11) we omitted the superscript M equaling 0 and used the fact

$$D_{00}^L(0, \theta, 0) = P_L(\cos \theta),$$

where P_L is the Legendre polynomial of order L . After transforming the volume integral in Eq. (11), we obtain

$$\begin{aligned} P_{n+1}^L(r, t) &= \mu_s \sqrt{\pi} \int_0^{r_{\max}} dr_1 \int_{x_{\min}}^1 dx_1 Y_{L0}(\theta_1) \\ &\times \exp[-(\mu_s + \mu_a)r_1] \\ &\times \sum_{\tilde{L}} \alpha_{\tilde{L}} P_n^{\tilde{L}}(r_2, t - r_1) P_{\tilde{L}}(\cos \theta_{12}), \end{aligned} \quad (12)$$

where

$$x_{\min} = \max\left(-1, \frac{r^2 - t^2 + 2tr_1}{2rr_1}\right) \quad (13)$$

follows from the inequality $|\mathbf{r} - \mathbf{r}_1| \leq t - r_1$ and

$$r_{\max} = \frac{r+t}{2}, \quad (14)$$

which follows from Eq. (13) and the fact that $x_{\min} \leq 1$. For details of further developments related to Eq. (12), it is useful to consult Ref. [3]. Note that the notation $P_n(r, t)$ in Ref.

[3] coincides with the notation $P_n^0(r, t)$ in this paper. Following the arguments of Ref. [3], one can prove that the function

$$P_n^L(r, t) \exp[(\mu_s + \mu_a)t] \quad (15)$$

is a homogeneous function of order $n-3$, so we arrive at the relation

$$P_n^L(r, t) = \exp[-(\mu_s + \mu_a)t] q_n^L\left(\frac{r}{t}\right) (\mu_s t)^{n-3}, \quad (16)$$

where we have introduced the functions $q_n^L(v)$. Using Eq. (16), we obtain the following recurrence relation for the quantities $q_n^L(v)$:

$$\begin{aligned} q_{n+1}^L(v) &= \frac{1}{2v} \int_0^1 dw w \sum_{\tilde{L}} \alpha_{\tilde{L}} (2\tilde{L}+1)^{1/2} \tilde{q}_n^{\tilde{L}}(w) \\ &\times \int \frac{\gamma_m(v, w)}{(1-v)/(1+w)} d\gamma \frac{\gamma^{n-1}}{1-\gamma} \\ &\times P_L\left(\frac{v^2 - w^2 \gamma^2 + (1-\gamma)^2}{2v(1-\gamma)}\right) \\ &\times P_{\tilde{L}}\left(\frac{v^2 - w^2 \gamma^2 - (1-\gamma)^2}{2w\gamma(1-\gamma)}\right), \end{aligned} \quad (17)$$

where

$$\gamma_m(v, w) = \begin{cases} \frac{1-v}{1-w} & \text{if } w < v, \\ \frac{1+v}{1+w} & \text{if } w > v. \end{cases} \quad (18)$$

Equation (17) enables one to calculate the functions $q_n^L(v)$ for arbitrary n and L starting from $n=0$ for each value of L :

$$q_0^L(v) = \frac{\mu_s^3}{4\pi} (2L+1)^{1/2} \delta(v-1). \quad (19)$$

In numerical calculations it is more convenient to apply Eq. (17) starting from $n=1$ than from $n=0$ because $q_0^L(v)$ contains a δ function. The functions $q_1^L(v)$ can be obtained analytically; we give them below for the case $\alpha_{\tilde{L}}=0$ with $\tilde{L} > 1$:

$$\begin{aligned} q_1^0(v) &= \frac{\mu_s^3}{4\pi v} \left\{ \ln \frac{1+v}{1-v} + \alpha_1 \sqrt{3} \left(v^2 \ln \frac{1+v}{1-v} - 2v \right) \right\}, \\ q_1^1(v) &= \frac{\sqrt{3} \mu_s^3}{16\pi v^2} \left\{ 2 \left[(v^2+1) \ln \frac{1+v}{1-v} - 2v \right] \right. \\ &\left. + \alpha_1 \sqrt{3} \left[(1+3v^4) \ln \frac{1+v}{1-v} - 2v(1+3v^2) \right] \right\}. \end{aligned} \quad (20)$$

To obtain the migration probability it is sufficient to know the quantities $q_n^L(v)$. Let $R(\hat{\mathbf{n}})$ be the photon flux distribution at the starting point normalized to unity. After expanding over spherical harmonics, we have

$$R(\hat{\mathbf{n}}) = \sum_L \beta_L Y_{L0}(\Omega_s) \frac{1}{\sqrt{4\pi}}. \quad (21)$$

Relation (21) implies that we have chosen the reference axis for Ω along the vector \mathbf{s} . The normalization condition yields $\beta_0=1$ since

$$\int d\Omega Y_{L0}(\Omega) = \begin{cases} \sqrt{4\pi} & \text{if } L=0, \\ 0 & \text{if } L>0. \end{cases} \quad (22)$$

To find the migration probability density along the vector \mathbf{r} , we expand $R(\hat{\mathbf{n}})$ with respect to this direction:

$$R(\hat{\mathbf{n}}) = \sum_{LM} \beta_L D_{M0}^L(0, (\hat{\mathbf{s}}, \mathbf{r}), 0) \frac{Y_{LM}(\Omega_{\mathbf{r}})}{\sqrt{4\pi}}. \quad (23)$$

Taking Eqs. (10) and (8) into account yields

$$P(\mathbf{r}, t) = P(\mathbf{r}, t) [R(\hat{\mathbf{n}})] = \sum_L \beta_L P_L(\cos(\hat{\mathbf{s}}, \mathbf{r})) P^L(r, t).$$

Using Eq. (16), we obtain the following practical expression for the migration probability density:

$$\begin{aligned} P(\mathbf{r}, t) &= \exp[-(\mu_s + \mu_a)t] \\ &\times \sum_{L=0}^{L_{\max}} \sum_{n=0}^{\infty} \beta_L P_L(\cos(\hat{\mathbf{s}}, \mathbf{r})) q_n^L\left(\frac{r}{t}\right) (\mu_s t)^{n-3}. \end{aligned} \quad (24)$$

where $(\hat{\mathbf{s}}, \mathbf{r})$ is the angle between \mathbf{s} and \mathbf{r} . The values of L over which the sum is calculated in Eq. (24) are those contained in the phase function expansion (5) (see next section for details). Since this function is not known quite exactly, it is sufficient to restrict oneself to the values $L=0, 1$. Higher values of L determine details of the phase function that are not important in applications and can be taken into account by a slight change in the parameters μ_s and α_1 [see Eq. (5)]. As for the sum over the number of scatterings, n , the number of terms effectively contributing depends on the values of r and t increasing with t and decreasing as r approaches t (draws nearer the light front; let us recall that the light velocity is assumed to be 1 in this paper). The essential point to stress here is that the diffusion approximation yields good enough results for large values of n . So the present approach is complementary to the diffusion approximation.

III. NUMERICAL ANALYSIS OF PHOTON MIGRATION

We performed calculations of the photon migration probabilities based on Eq. (24) in the preceding section. Toward this end, the functions $q_n^L(v)$ were first calculated using recurrence relations (17) and stored in computer memory. Values were calculated for n up to 30, which enables one to calculate probability densities for $\mu_s t \leq 15$ with an accuracy to within 1%. Figures 2 and 3 plot the functions $q_n^0(v)$ and $q_n^1(v)$. We assumed in the calculations that the expansion of the phase function in Eq. (5) contained the terms with $L=0$ and $L=1$ only. Therefore the only parameter specifying the phase function is α_1 . Its positive definiteness implies

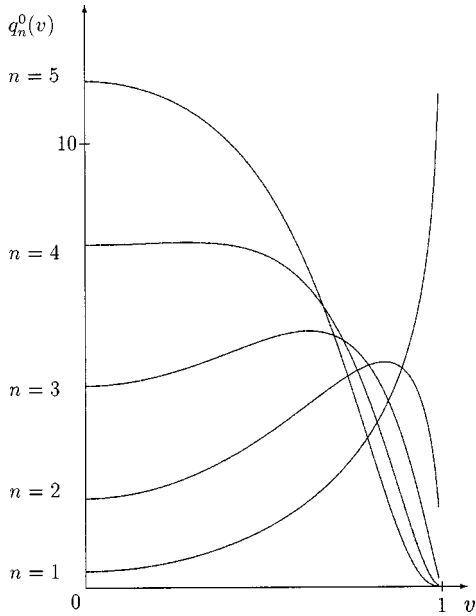


FIG. 2. Functions $q_n^0(v)$ for some values of n .

that $|\alpha_1| \leq 1/\sqrt{3}$. Here $\alpha_1=0$ yields isotropic scattering, whereas the value $\alpha_1=1/\sqrt{3}$ corresponds to the case with no backward scattering. Since scattering into the forward hemisphere dominates, values of $\alpha_1 \geq 0$ are physically sensible. The second parameter we used in our calculations was the scattering coefficient μ_s . We ignored photon absorption, setting $\mu_a=0$. Figure 4 depicts photon travel through the medium that we used in the calculations. At the initial point O the photon is directed along the z axis as is the case for laser light injection. The photon is detected in the plane normal to this axis and offset from the point O by the distance d . The first scattering occurs at the point N . So the probability of migration to the detection point can be represented as

$$P_M(t, d, s) = \mu_s \int_0^{z_{\max}} dz \exp(-\mu_s z) P(\mathbf{r}_M - \mathbf{r}_N, t - z), \quad (25)$$

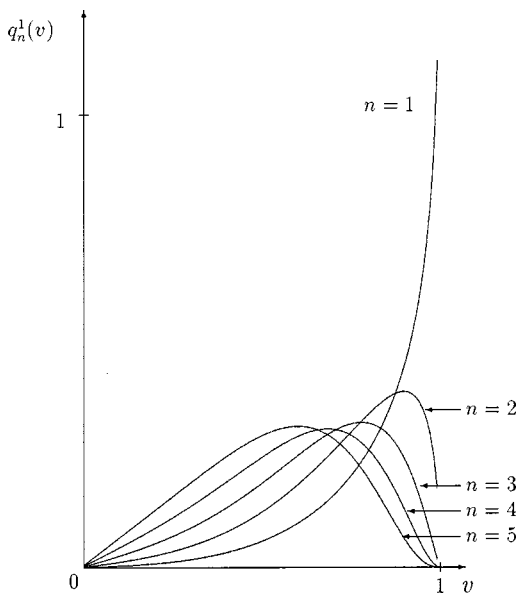


FIG. 3. Functions $q_n^1(v)$ for some values of n .

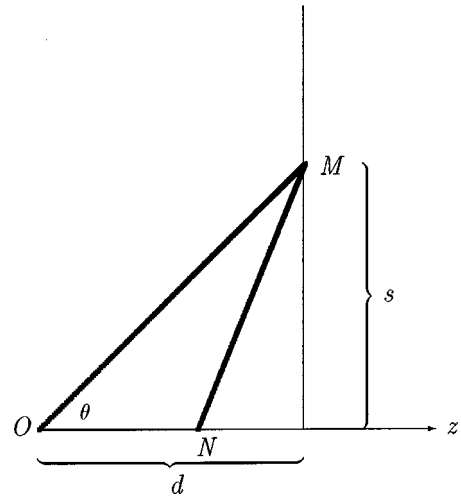


FIG. 4. Scheme of photon travel for which the migration probabilities were calculated.

where s is the distance between the detection point and the z axis. z_{\max} in Eq. (25) is defined by the inequality

$$|\mathbf{r}_M - \mathbf{r}_N| < t - z, \quad (26)$$

which yields

$$z_{\max} = \frac{t + d}{2} - \frac{s^2}{2(t - d)}. \quad (27)$$

The migration probability $P(\mathbf{r}_M - \mathbf{r}_N, t - z)$ entering into Eq. (25) is calculated using formula (24). The parameters β_L specifying the angle distribution of the photon scattered at the point N should be set equal to α_L appearing in Eq. (5) for the phase function. Table I summarizes the results of our calculations. For each value of d (the z coordinate of the detection plane), we computed the migration densities for various values of s (distance from the detection point to the z axis). The values of s are given in the first line of each segment of the table. Clearly, $s \leq \sqrt{t^2 - d^2}$. In all cases the total migration time $t=15$. The second line contains exact values of the migration probability densities for anisotropic scattering with $\mu_s=1$ and $\alpha_1=0.5$. The third line gives the best-fit data obtained if the scattering is considered to be isotropic, the fitting parameter being the scattering coefficient μ_s . The best-fit value of μ_s is given above each segment of the table. We considered two classes of detection planes: forward lying and rear lying. The latter ones are located behind the light source and can be reached by diffusely reflected photons only. The criterion we used in the fitting procedure is the root-mean-square relative error given by the formula

$$\delta = \left[\sum_{k=0}^{10} \frac{1}{11} \left(\frac{P_M^{\text{exact}}(t, d, s_k) - P_M^{\text{isotropic}}(t, d, s_k)}{P_M^{\text{exact}}(t, d, s_k)} \right)^2 \right]^{1/2}, \quad (28)$$

with $s_k=k$. The values of δ corresponding to the best fit are given together with the μ_s values. As can be seen from Table I, an approach with isotropic scattering with an effective scattering coefficient can yield a very poor approximation only. The approximation gets worse for more distant detection planes. The reason is obvious: in this case the first transmitted photons play a more important role, but they experience a smaller number of scatterings on average and the

TABLE I. Probabilities of photon migration according to the scheme of Fig. 4.

$d = 11, \mu_s = 0.91, \delta = 54\%$											
s	0	1	2	3	4	5	6	7	8	9	10
Exact	4.5×10^{-5}	4.2×10^{-5}	3.6×10^{-5}	2.7×10^{-5}	1.7×10^{-5}	9.5×10^{-6}	4.3×10^{-6}	1.5×10^{-6}	3.6×10^{-7}	5.0×10^{-8}	1.5×10^{-9}
Fit	2.6×10^{-5}	2.4×10^{-5}	1.9×10^{-5}	1.3×10^{-5}	7.3×10^{-6}	3.6×10^{-6}	1.5×10^{-6}	5.4×10^{-7}	1.5×10^{-7}	2.9×10^{-8}	2.5×10^{-9}
$d = 10, \mu_s = 0.82, \delta = 28\%$											
s	0	1	2	3	4	5	6	7	8	9	10
Exact	9.7×10^{-5}	9.3×10^{-5}	8.0×10^{-5}	6.2×10^{-5}	4.3×10^{-5}	2.6×10^{-5}	1.3×10^{-5}	5.5×10^{-6}	1.7×10^{-6}	3.9×10^{-7}	4.8×10^{-8}
Fit	8.7×10^{-5}	8.2×10^{-5}	6.7×10^{-5}	4.9×10^{-5}	3.1×10^{-5}	1.7×10^{-5}	8.4×10^{-6}	3.5×10^{-6}	1.2×10^{-6}	3.5×10^{-7}	7.1×10^{-8}
$d = 5, \mu_s = 0.69, \delta = 6.9\%$											
s	0	1	2	3	4	5	6	7	8	9	10
Exact	8.8×10^{-4}	8.5×10^{-4}	7.6×10^{-4}	6.3×10^{-4}	4.9×10^{-4}	3.4×10^{-4}	2.2×10^{-4}	1.3×10^{-4}	6.3×10^{-5}	2.7×10^{-5}	9.3×10^{-6}
Fit	9.4×10^{-4}	9.0×10^{-4}	7.9×10^{-4}	6.4×10^{-4}	4.8×10^{-4}	3.3×10^{-4}	2.0×10^{-4}	1.1×10^{-4}	5.9×10^{-5}	2.7×10^{-5}	1.1×10^{-5}
$d = -5, \mu_s = 0.76, \delta = 5.9\%$											
s	0	1	2	3	4	5	6	7	8	9	10
Exact	3.1×10^{-4}	3.0×10^{-4}	2.7×10^{-4}	2.2×10^{-4}	1.7×10^{-4}	1.2×10^{-4}	7.3×10^{-5}	4.1×10^{-5}	2.0×10^{-5}	8.5×10^{-6}	2.9×10^{-6}
Fit	3.3×10^{-4}	3.2×10^{-4}	2.8×10^{-4}	2.3×10^{-4}	1.7×10^{-4}	1.1×10^{-4}	6.9×10^{-5}	3.8×10^{-5}	1.9×10^{-5}	8.4×10^{-6}	3.2×10^{-6}
$d = -10, \mu_s = 0.91, \delta = 32\%$											
s	0	1	2	3	4	5	6	7	8	9	10
Exact	7.1×10^{-6}	6.8×10^{-6}	5.8×10^{-6}	4.4×10^{-6}	3.0×10^{-6}	1.7×10^{-6}	8.7×10^{-7}	3.6×10^{-7}	1.1×10^{-7}	2.5×10^{-8}	3.2×10^{-9}
Fit	5.0×10^{-6}	4.7×10^{-6}	4.0×10^{-6}	3.0×10^{-6}	2.0×10^{-6}	1.1×10^{-6}	5.7×10^{-7}	2.5×10^{-7}	8.8×10^{-8}	2.5×10^{-8}	4.8×10^{-9}
$d = -11, \mu_s = 1.01, \delta = 60\%$											
s	0	1	2	3	4	5	6	7	8	9	10
Exact	2.0×10^{-6}	1.9×10^{-6}	1.6×10^{-6}	1.1×10^{-6}	7.3×10^{-7}	3.9×10^{-7}	1.8×10^{-7}	6.1×10^{-8}	1.5×10^{-8}	2.1×10^{-9}	5.8×10^{-11}
Fit	8.3×10^{-7}	7.8×10^{-7}	6.3×10^{-7}	4.5×10^{-7}	2.8×10^{-7}	1.5×10^{-7}	6.5×10^{-8}	2.3×10^{-8}	6.6×10^{-9}	1.3×10^{-9}	1.0×10^{-10}

anisotropy is not masked as much as it is for diffusive photons.

IV. CONCLUDING REMARKS

Let us summarize the results presented in this paper. We have given a method for describing migration probabilities in an infinite, homogeneous medium scattering photons anisotropically. The result is given in the form of an expansion over the number of scatterings the photon undergoes as it migrates in the medium. The expansion converges rapidly, and the error originating from its cutoff can be easily estimated. The number of terms that need to be included decreases as one approaches the light front, i.e., for the first transmitted photons. For diffusive photons, where the number of scatterings is large, the diffusion approximation becomes a reliable approach. Thus one can say that our method builds a bridge between the two extreme cases: early transmitted photons and diffusive photons covering the region most difficult for investigation (see Ref. [4], for example). Let us briefly discuss how the present work relates to some other investigations in this field. First of all, note Ishimaru's [6] and Furutsu's [7] theories. In these papers differential equations for light intensity are derived which describe light propagation more precisely than the standard diffusion equation does. The main approximation used in these theories is the linear dependence of the light intensity on the cosine of

the angle determining the propagation direction (see Ref. [8]). Both approaches substantially improve the diffusion approximation. Nevertheless, it is clear that they are not sufficient near the light front where the forward direction of light propagation strongly dominates. A more accurate account of the problem is given in Gershenson's paper [9] where an equation is obtained that is similar to the diffusion equation but includes the angular distribution of the light intensity. This equation is expected to predict the intensity of multiple scattering at earlier times and shorter distances than the diffusion equation can. Note that the approach of this paper is difficult to apply in the case of a strongly peaked phase function because of the poorly converging expansion over spherical harmonics. That is why the so-called two-stream theories are useful in which the forward and backward scattering is assumed to dominate in course of light propagation (see Ref. [1]). The present method can be also applied to bounded media using the modified Monte Carlo method described in Ref. [5]. Nevertheless, a generalization of the present approach to bounded media would be very desirable and would substantially increase its practical value. Some attempts of this kind are currently being undertaken.

ACKNOWLEDGMENT

The authors are grateful to the staff of the Centro de Cálculo de la Universidad de Cantabria for their kind help in performing the calculations.

- [1] D. J. Durian and J. Rudnick, *J. Opt. Soc. Am. A* **14**, 235 (1997).
- [2] K. M. Yoo, Feng Liu, and R. R. Alfano, *Phys. Rev. Lett.* **64**, 2647 (1990).
- [3] V. N. Fomenko and F. M. Shvarts, *Proc. SPIE* **3194**, 334 (1997).
- [4] A. Ishimaru, *Wave Propagation and Scattering in Random Media* (Academic, New York, 1987).
- [5] F. M. Shvarts and V. N. Fomenko, *Proc. SPIE* **3194**, 343 (1997).
- [6] A. Ishimaru, *J. Opt. Soc. Am.* **68**, 1045 (1978).
- [7] K. Furutsu, *J. Opt. Soc. Am.* **70**, 360 (1980).
- [8] S. Kumar, K. Mitra, and Y. Yamada, *Appl. Opt.* **35**, 3372 (1996).
- [9] M. Gershenson, *Phys. Rev. E* **59**, 7178 (1999).